Enhancement of strong-electromagnetic-field ionization in a constant magnetic field

V. M. Rylyuk*
National Academy of Sciences of Ukraine "Hydroacoustic Branch of Geophysical Institute of NAS of Ukraine", Preobrazhenskaya 3, 65082 Odessa, Ukraine

(Received 1 July 2019; revised manuscript received 18 October 2019; published 15 November 2019)

The tunneling and multiphoton ionization of a weakly bound level in an intense laser field of an arbitrary polarization and a constant uniform magnetic field, under the condition when the frequency ω of a laser field coincides with the cyclotron frequency ω_H, are discussed in the quasistationary quasienergy state (QQES) formalism framework. The integral equation is derived for the complex quasienergy of the photoelectron, on the basis of the exact solution of the Schrödinger equation for an electron moving in an arbitrary electromagnetic wave and a constant magnetic field, obtained in Rylyuk [Phys. Rev. A **93**, 053404 (2016)]. Simple analytical expressions for ionization rates in the tunneling and the multiphoton regimes by using the saddle-point method are derived and discussed. Using the "imaginary-time" method, the extremal subbarrier trajectory, the barrier width, and the emission angle of photoelectrons are considered. We theoretically demonstrate that when the frequency of a left polarized laser field coincides with the cyclotron frequency, the constant magnetic field does not stabilize the bound level, which leads to an enhancement of the ionization rate as compared to when the magnetic field is absent.

DOI: 10.1103/PhysRevA.100.053409

I. INTRODUCTION

Over the past 30 years significant progress has been made in the development of lasers capable of producing ultrashort and strong pulses with durations of the order of femtoseconds (10^{-15} s) and intensities of the order of 10^{14}–10^{15} W/cm^2. In this regard, of unabated interest are the phenomena related to the interaction of high-intensity laser radiation with atoms and ions [1–17]. Ionization is one of these effects which characterizes the interaction of laser radiation with matter. The basic concepts of the theory of ionization were developed by Keldysh [18]. In Ref. [18] was shown that the character of the ionization depends on the magnitude of the Keldysh parameter

$$\gamma = \frac{\kappa\omega}{eF}, \tag{1}$$

where $\kappa = \sqrt{2m|E_0|}$ is the inner-atomic momentum ($|E_0|$ is the binding energy of the level), ω is the laser frequency, F is the magnitude of the perturbing field, and m and e are the electron mass and elementary charge, respectively. Tunneling ionization of atomic states takes place when $\gamma \ll 1$ and the multiphoton regime is realized when $\gamma \gg 1$. The ionization in constant electric and magnetic fields was considered in Refs. [19–21] within the adiabatic approach. These studies showed that the ionization rate decreases as the magnetic field increases. This effect is explained by the increase of the length of the electron subbarrier trajectory. In the presence of a magnetic field, the electron moves along a helix and its trajectory becomes longer, which impedes penetration of the electron through the barrier. In Refs. [22–29] was developed the quasistationary quasienergy state (QQES) formalism that allows one to find the exact solution of a full nonstationary problem of the decay of a weakly bound level in an elliptically polarized laser field with an arbitrary intensity and frequency. Further, in Refs. [30–32], within the framework of the QQES formalism, was considered the atomic ionization in an intense laser radiation field of an arbitrary polarization and a constant magnetic field. The questions considered above were also expounded in reviews [4,33–37].

The aim of this paper is to consider the ionization of a weakly bound level in an intense monochromatic elliptically polarized laser beam propagating at an arbitrary angle to the constant magnetic field in the case when the frequency ω of an elliptical laser field and the cyclotron frequency ω_H are equal. For this purpose, using the QQES formalism, the saddle-point, and the "imaginary-time" methods [38,39], we derive ionization rates and the extremal subbarrier trajectory of the electron. We analyze in detail analytical expressions for ionization rates, the barrier width, and the emission angle of photoelectrons, in the tunneling and multiphoton limits. Our consideration is also complemented by numerical calculations of ionization rates and "stabilization factors" for neutral atoms of hydrogen and helium in the field of a titanium-sapphire laser. Our calculations show that contrary to the widespread view, the constant magnetic field in the presence of an electromagnetic wave, when $\omega = \omega_H$, does not always tend to suppress the ionization of the bound level. So, in the case of a right polarized laser field the constant magnetic field suppresses the ionization, i.e., stabilizes the bound level. The reason for this is that a right polarized laser field and the constant magnetic field rotate the electron in the same direction (corotating electron). As a result the subbarrier trajectory of the electron elongates, reducing the chance of the electron penetrating the barrier. On the contrary, in the case of a left

*rvm@onu.edu.ua

polarized laser field, when the constant magnetic field and the electromagnetic wave rotate the electron in the opposite directions (counterrotating electron) and the frequency ω of the laser field is equal to the cyclotron frequency ω_H, the constant magnetic field does not stabilize the bound level, which leads to an enhancement of the ionization rate as compared to the case when the magnetic field is absent. In Ref. [40] was shown that in the case of a linearly polarized electromagnetic wave, under the condition $\omega = \omega_H$, the constant magnetic field always stabilizes the bound level.

It should be noted that the ionization induced by an electromagnetic wave and a magnetic field is also of great practical importance. The method of magnetic cumulation (explosion-assisted compression of an axial magnetic field), proposed by Sakharov in [41,42], made it possible to obtain magnetic fields $H \simeq 15$–25 MG. A strong magnetic field with an amplitude $\sim$50 MG was generated in overdense laser-produced plasmas (e.g., at the critical electron number density $n_e \sim 10^{21}$ cm^{-3}) by a laser pulse with the wavelength $\sim$1.054 μm of duration $\tau_0 \sim 1$ ps and intensity $\sim 10^{20}$ W/cm^2 [43]. Magnetic fields in the range 340–460 MG were obtained in a solid target irradiated with a high-intensity ($\sim 10^{19}$ W/cm^2) picosecond laser pulse [44,45]. Ultrastrong-magnetic-field strengths of 0.7 ± 0.1 GG in the overdense plasma are produced during intense ($\sim 10^{20}$ W/cm^2) laser interaction experiments with solids [46]. The magnitudes of magnetic fields generated in these experiments could soon approach those needed for testing astrophysical models of neutron stars and white dwarfs. For instance, at the surface of white dwarf star magnetic fields ranging from 2 MG to roughly 1000 MG may be observed [47]. White dwarf stars are remarkable because it is possible to observe their optical spectra [47,48] allowing one to study the effect of large electric and magnetic fields on the atomic levels, primarily for the atoms of hydrogen and helium.

The paper is organized as follows. Section II represents analytical results of an elliptically polarized laser beam propagating at an arbitrary angle to the constant magnetic field. In Sec. III we derive the subbarrier trajectory, barrier width, and emission angle of photoelectrons. In Sec. IV we analyze the results of numerical calculations for ionization rates and stabilization factors. Section V concludes the work.

II. ANALYTICAL RESULTS OF AN ELLIPTICALLY POLARIZED LASER BEAM PROPAGATING AT AN ARBITRARY ANGLE TO THE CONSTANT MAGNETIC FIELD

Now, consider an elliptically polarized monochromatic laser beam of frequency ω, which propagates at an angle θ to the constant magnetic field $\boldsymbol{H}$ (we choose the direction of $\boldsymbol{H}$ as the z axis). The components of its vector potential $\boldsymbol{A}(t) = (A_x(t), A_y(t), A_z(t))$ are

$$A_x(t) = -\frac{F}{\omega}\cos(\theta)\sin\omega t, \quad A_y(t) = g\frac{F}{\omega}\cos\omega t,$$
$$A_z(t) = -\frac{F}{\omega}\sin(\theta)\sin\omega t, \tag{2}$$

where F is the laser field amplitude and g is the ellipticity of the laser field ($-1 \leqslant g \leqslant +1$). The wave function $\Psi_\epsilon(\boldsymbol{r}, t) = \exp(-i\epsilon t/\hbar)\Phi_\epsilon(\boldsymbol{r}, t)$ of the electron moving in the field of potential $U(\boldsymbol{r})$ and in the net electromagnetic field produced by the electromagnetic wave and the constant magnetic field reads

$$\Phi_\epsilon(\boldsymbol{r}, t) = \int_{-\infty}^{t} dt' e^{i\epsilon(t-t')/\hbar} \int d\boldsymbol{r}'\, G(\boldsymbol{r}, t; \boldsymbol{r}', t')U(\boldsymbol{r}')\Phi_\epsilon(\boldsymbol{r}', t'), \tag{3}$$

where ϵ is the complex quasienergy and $G(\boldsymbol{r}, t; \boldsymbol{r}', t')$ is the retarded Green's function for the electron moving in the laser pulse (2) and the constant magnetic field $\boldsymbol{H}$, which was derived in Ref. [30] [see Eq. (5)]. For calculating the complex quasienergy $\epsilon = E - i\Gamma$ of the electron we use the QQES formalism. In this approach the real and imaginary parts of the complex quasienergy determine the Stark shift $\Delta\epsilon = E - E_0$ and the laser field-induced width $\hbar\Gamma$ of the bound level. In the zero-range potential model the wave function $\Phi_\epsilon(\boldsymbol{r}, t)$ from Eq. (3), for the electron in the s state, satisfies the boundary condition at $r \to 0$ [22,23,49,50]:

$$\Phi_\epsilon(\boldsymbol{r}, t) \simeq \left(\frac{1}{r} - \frac{1}{a} - 2i\frac{e}{\hbar c}\frac{\boldsymbol{r}\boldsymbol{A}_f(t)}{r}\right) f_\epsilon(t) + O(r),$$
$$f_\epsilon(t) = f_\epsilon\left(t + \frac{2\pi}{\omega}\right), \tag{4}$$

and the following relation

$$U(\boldsymbol{r})\Phi_\epsilon(\boldsymbol{r}, t) = -2\pi\delta(\boldsymbol{r}) f_\epsilon(t), \tag{5}$$

where $a = \hbar/\sqrt{2m|E_0|}$ is the scattering length, E_0 is the energy of the electron bound by the zero-range potential alone, $\boldsymbol{A}_f(t)$ is the sum of the vector potentials of the laser pulse and the constant magnetic field, and $f_\epsilon(t)$ is the new unknown function. Using Eqs. (4) and (5) we get from Eq. (3) the closed equation for the complex quasienergy (see details in Refs. [30,32])

$$\beta \simeq 1 + \frac{1}{2\sqrt{\pi i\lambda}}\frac{1}{\pi}\int_0^{\pi} d\tau \int_0^{\infty} \frac{dt}{t^{3/2}} \exp(-i\lambda\beta^2 t)$$
$$\times \left\{\frac{\omega_0 t}{2\sin(\omega_0 t/2)} \exp\left[i\lambda S(\tau, t)\right] - 1\right\}, \tag{6}$$

where $\beta = \sqrt{-\epsilon/|E_0|}$ describes the alteration of the electron energy by the laser and magnetic fields, $\omega_0 = \omega_H/\omega$ ($\omega_H = |e|H/(mc)$ is the cyclotron frequency), $\lambda = |E_0|/(\hbar\omega)$ is the multiquantum parameter, $S(\tau, t) = \lim_{\boldsymbol{r},\boldsymbol{r}'\to \boldsymbol{0}} S(\boldsymbol{r}, \tau; \boldsymbol{r}', \tau - t)$, and the classical action $S(\boldsymbol{r}, \tau; \boldsymbol{r}', t)$ is determined by Eqs. (A19) and (A20) in Ref. [30].

In this paper we consider the situation when $\omega = \omega_H$ ($\omega_0 = 1$). For getting some analytical results we limit ourselves by the case of weak electric $F \ll F_0$ ($F_0 = \kappa^3$ is the inner-atomic field; for the ground state of the hydrogen atom $F_0 = m^2e^5/\hbar^4 = 5.14 \times 10^9$ V cm^{-1} is the electric field at the first Bohr orbit) and magnetic $H \ll H_0$ ($H_0 = \kappa^2 = 2.35 \times 10^9$ G for the H atom) fields, when the inequality $\lambda \gg 1$ holds. Under these conditions the tunneling of an electron from under the barrier has the quasiclassical character. Transforming the integral in Eq. (6) over t into one in the complex plane $x = -i\omega_H t$ and applying the standard saddle-point method at $\lambda = \lambda_H \gg 1$, we obtain the expressions for the width $\hbar\Gamma$

and the shift $E - E_0$ of the bound s electron level in the quasiclassical approximation, in the case when $\omega = \omega_H$,

$$\Gamma \simeq \frac{\omega_H}{2\sqrt{2x_0}\sinh(x_0)}\frac{1}{\sqrt{|F''(x_0)|}}\exp\left[-2\lambda_H F(x_0)\right], \tag{7}$$

$$E \simeq |E_0|\left\{-1 - \frac{1}{4}\left(\frac{F}{F_0}\right)^2\left[1 + \frac{7}{48\lambda_H^2}(3 - g^2) - \frac{7}{12}\frac{g}{\lambda_H}\frac{H}{H_0} + \frac{13}{2}\left(\frac{F}{F_0}\right)^2\right] + \frac{1}{12}\left(\frac{H}{H_0}\right)^2 - \frac{5}{144}\left(\frac{H}{H_0}\right)^4 + \frac{1}{2}\left(\frac{FH}{F_0H_0}\right)^2\right\}, \tag{8}$$

where $\lambda_H = |E_0|/(\hbar\omega_H)$ is the magnetic multiquantum parameter determining the minimal number of photons necessary for the ionization and $F(x_0) = \frac{i}{2}[S(\tau = t/2, t) + \beta^2 t]_{t=-2ix_0}$:

$$F(x_0) = \left(1 + \frac{4 + \mathcal{G}^2(g,\theta)}{8\gamma_H^2}\right)x_0 - \frac{4 - \mathcal{G}^2(g,\theta)}{16\gamma_H^2}\sinh(2x_0) - \frac{\mathcal{G}^2(g,\theta)}{4\gamma_H^2}x_0^2\coth(x_0). \tag{9}$$

In Eqs. (7) and (9) $\gamma_H = \sqrt{2|E_0|}\omega_H/F$ is the magnetic Keldysh parameter and x_0 is the saddle point, which is determined by the condition $F'(x_0) = 0$, i.e., by the saddle-point equation

$$\mathcal{G}^2(g,\theta)\left[x_0^2 - [1 - x_0\coth(x_0)]^2\right] + [4 - \mathcal{G}^2(g,\theta)]\sinh^2(x_0) = 4\gamma_H^2, \tag{10}$$

where $\mathcal{G}(g,\theta) = g + \cos(\theta)$. Note that x_0 has a simple physical interpretation: $t_0 = -ix_0/\omega_H$ is the time of the subbarrier motion of the electron. The expressions (7) and (8) are the quasiclassical ionization rate and the level shift for an s electron in a zero-range potential under the influence of the elliptically polarized laser field (2) at $\omega = \omega_H$ and the constant magnetic field $\boldsymbol{H}$. The real part E in Eq. (8) of the quasienergy contains the contributions $\sim F$ and H from the Stark and the Zeeman effects, and the cross terms $\sim FH$. One sees from Eq. (8) that the term in the quadratic brackets, which is proportional to $g(H/H_0)$, increases the energy in the case of a right polarized wave and decreases it in the case of a left polarized wave. Further throughout the paper we will use the atomic units: $e = m = \hbar = 1$.

In the tunneling limit, where the inequality $\gamma_H \ll 1$ holds, the saddle point x_0 in Eq. (10) can be written in the following analytical form:

$$x_0 \simeq \gamma_H\left\{1 - \frac{\gamma_H^2}{6}\left(1 - \frac{\mathcal{G}^2(g,\theta)}{3}\right) + \frac{3}{40}\left[1 - \frac{22}{27}\mathcal{G}^2(g,\theta)\left(1 - \frac{35}{198}\mathcal{G}^2(g,\theta)\right)\right]\gamma_H^4\right\}. \tag{11}$$

Then, from Eq. (7), for the ionization rate we obtain

$$\Gamma \simeq |E_0|\frac{F}{2}P(\gamma_H, g, \theta)\exp\left\{-\frac{2}{3F}f(\gamma_H, g, \theta)\right\}, \tag{12}$$

where the exponential factor is

$$f(\gamma_H, g, \theta) \simeq 1 - \frac{\gamma_H^2}{10}\left(1 - \frac{\mathcal{G}^2(g,\theta)}{3}\right) + \frac{9}{280}\left[1 - \frac{22}{27}\mathcal{G}^2(g,\theta)\left(1 - \frac{35}{198}\mathcal{G}^2(g,\theta)\right)\right]\gamma_H^4, \tag{13}$$

and the preexponential factor reads

$$P(\gamma_H, g, \theta) \simeq 1 - \frac{\gamma_H^2}{6}\left(1 - \frac{7}{60}\gamma_H^2\right) + \frac{13}{120}\left[1 - \frac{56}{117}\mathcal{G}^2(g,\theta)\left(1 - \frac{5}{42}\mathcal{G}^2(g,\theta)\right)\right]\gamma_H^4. \tag{14}$$

Equations (11)–(14) show that the ionization rate (12) depends on the ellipticity g and the angle θ only via the factor $\mathcal{G}(g,\theta) = g + \cos(\theta)$. The term $\sim 1 - \gamma_H^2(1 - 7\gamma_H^2/60)/6$ in the preexponential factor describes the diamagnetic shift in the ionization rate.

In the multiphoton regime, i.e., for $\gamma_H \gg 1$ and at $\mathcal{G}(g,\theta) \neq 2$, the saddle point reads

$$x_0 \simeq \ln\left(\frac{4\gamma_H^2}{\sqrt{4 - \mathcal{G}^2(g,\theta)}}\right), \tag{15}$$

and the ionization rate (12) can be represented in the form

$$\Gamma \simeq \frac{\sqrt{2}}{16}\frac{F}{\sqrt{|E_0|}}\sqrt{\frac{4 - \mathcal{G}^2(g,\theta)}{x_0}}\left[\frac{\mathrm{e}}{64}\frac{(4 - \mathcal{G}^2(g,\theta))F^4}{E_0^2\omega_H^4}\right]^{\lambda_H} \times \exp\left\{\frac{\mathcal{G}^2(g,\theta)F^2}{4\omega_H^3}x_0^2\right\}, \tag{16}$$

where e is the Euler number. In the special case, when a right circularly polarized laser beam ($g = +1$) propagates parallel ($\theta = 0$) to the magnetic field $\boldsymbol{H}$, i.e., at $\mathcal{G}(g,\theta) = 2$, the saddle point in the multiphoton regime is

$$x_0 \simeq \frac{\gamma_H^2}{2}, \tag{17}$$

and the ionization rate may be written as

$$\Gamma \simeq \frac{F}{2\sqrt{|E_0|}}\gamma_H\exp\left\{-\frac{\gamma_H^2}{2}(1 + \lambda_H)\right\}. \tag{18}$$

As follows from Eq. (18), the constant magnetic field causes the exponential reduction of the ionization rate. This effect can be explained by the distortion of the subbarrier trajectory due to the screwlike electron motion. As a result, the subbarrier trajectory of the electron in a right circularly polarized laser field becomes longer and the ionization rate decreases.

III. BARRIER WIDTH AND EMISSION ANGLE OF PHOTOELECTRONS

Within the framework of the imaginary-time method we can calculate the width of the barrier in the case when $\omega = \omega_H$:

$$b(g,\theta) = |\boldsymbol{r}(0)|, \tag{19}$$

where $\boldsymbol{r}(x) = (r_x(x), r_y(x), r_z(x))$ is the extremal subbarrier trajectory of the electron. In order to determine this trajectory we use the imaginary-time method. Being a generalization of the well-known method of complex classical trajectories considered by Landau [51,52] in the case of time-dependent fields, the imaginary-time method describes the tunneling transition of an electron from a bound state to the continuum using the classical equations of motion but with an imaginary "time." Integrating the equations of motion

$$\ddot{\boldsymbol{r}} = \frac{1}{c}\partial \boldsymbol{A}(t)/\partial t - \frac{1}{c}[\dot{\boldsymbol{r}}, \boldsymbol{H}], \tag{20}$$

where $\boldsymbol{A}(t)$ is the vector potential (2) at $\omega = \omega_H$ and $\boldsymbol{H}$ is the constant magnetic field, with the initial condition

$$\boldsymbol{r}(x_0) = \boldsymbol{0} \tag{21}$$

and the boundary conditions

$$\text{Im}\, \boldsymbol{r}(0) = \text{Im}\, \dot{\boldsymbol{r}}(0) = \boldsymbol{0}, \tag{22}$$

we obtain the following result for the extremal subbarrier trajectory of the electron in the case when $\omega = \omega_H$:

$$\begin{aligned} r_x(x) = {} & \frac{F}{2\omega_H^2}\{[\cosh(x) - \cosh(x_0)] \\ & \times [\mathcal{G}(g,\theta)(1 - x_0\coth(x_0)) - 2g] \\ & + \mathcal{G}(g,\theta)[x\sinh(x) - x_0\sinh(x_0)]\}, \\ r_y(x) = {} & \frac{iF}{2\omega_H^2}\mathcal{G}(g,\theta)\{x\cosh(x) - x_0\cosh(x_0) \\ & - x_0\coth(x_0)[\sinh(x) - \sinh(x_0)]\}, \\ r_z(x) = {} & \frac{F}{\omega_H^2}\sin(\theta)[\cosh(x) - \cosh(x_0)], \end{aligned} \tag{23}$$

where the saddle point x_0 is determined by Eq. (10). Equation (22) means that the extremal trajectory at $t = 0$ is real and further describes the motion of the electron at infinity in the classically allowed region.

In the adiabatic limit, i.e., for $\gamma_H \ll 1$, the width of the barrier (19) is

$$b(g,\theta) \simeq \frac{\kappa^2}{2F}\left\{1 - \frac{\gamma_H^2}{4}\left[1 - \frac{1}{9}\{4g^2 + [5g + \cos(\theta)]\cos(\theta)\}\right]\right\}, \tag{24}$$

and in the multiphoton regime, i.e., for $\gamma_H \gg 1$, the width of the barrier may be written as

$$b(g,\theta) \simeq \frac{\kappa}{\omega_H}\sqrt{\frac{[g - \cos(\theta)]^2 + 4\sin^2(\theta)}{4 - [g + \cos(\theta)]^2}}. \tag{25}$$

In the special case, when a right circularly polarized laser beam ($g = +1$) propagates parallel ($\theta = 0$) to the constant magnetic field $\boldsymbol{H}$, the width of the barrier is

$$b(g = +1, \theta = 0) \simeq \frac{\kappa^2}{2F}. \tag{26}$$

When a left circularly polarized laser beam ($g = -1$) propagates parallel ($\theta = 0$) to the constant magnetic field $\boldsymbol{H}$, the width of the barrier reads

$$b(g = -1, \theta = 0) \simeq \frac{\kappa}{\omega_H}. \tag{27}$$

As can be seen from Eqs. (26) and (27), $b(g = +1, \theta = 0)/b(g = -1, \theta = 0) \sim \gamma_H \gg 1$, i.e., the barrier width in the case of a right circular laser field is greater than in a left circular laser field. This means that the ionization rate in a left polarized laser pulse is greater than in a right polarized laser pulse. The reason for this is that a left circularly polarized laser field rotates the electron against the constant magnetic field while a right circularly polarized laser pulse and the constant magnetic field rotate the electron at the same direction, i.e., a counterrotating electron has significantly better chances to penetrate the barrier than a corotating electron.

At the moment when the electron overcomes the barrier,

$$r_y(0) = 0, \quad \tan(\varphi) = \frac{r_x(0)}{r_z(0)}, \tag{28}$$

where φ is the emission angle of the electron ejected from under the barrier. In the adiabatic limit ($\gamma_H \ll 1$), in the case when $\omega = \omega_H$,

$$\varphi \simeq \frac{\pi}{2} - \theta - \frac{\gamma_H^2}{12}[g + \cos(\theta)]\sin(\theta), \tag{29}$$

or for small angles $\theta \ll 1$

$$\varphi \simeq \frac{\pi}{2} - \left[1 + \frac{\gamma_H^2}{12}(1 + g)\right]\theta. \tag{30}$$

Equations (29) and (30) show that the photoelectron moves along the electric field during subbarrier motion. In the antiadiabatic limit ($\gamma_H \gg 1$), and if $g \neq +1$ and $\theta \neq 0$, i.e., at $\mathcal{G}(g,\theta) \neq 2$, the emission angle is

$$\begin{aligned} \varphi \simeq {} & -\arctan\left(\frac{g - \cos(\theta)}{2\sin(\theta)}\right) \\ & - \frac{\sin(\theta)}{2\gamma_H}\frac{\mathcal{G}(g,\theta)\sqrt{4 - \mathcal{G}^2(g,\theta)}}{[g - \cos(\theta)]^2 + 4\sin^2(\theta)}\ln\left(\frac{4 - \mathcal{G}^2(g,\theta)}{16\gamma_H^2}\right), \end{aligned} \tag{31}$$

or for small angles $\theta \ll 1$

$$\begin{aligned} \varphi \simeq {} & \frac{\pi}{2}\text{sgn}[\cos(\theta) - g] - \frac{2}{1 - g}\left[1 + \frac{\mathcal{G}(g,\theta)}{4\gamma_H(1 - g)}\sqrt{4 - \mathcal{G}^2(g,\theta)}\right. \\ & \left.\times \ln\left(\frac{4 - \mathcal{G}^2(g,\theta)}{16\gamma_H^2}\right)\right]\theta. \end{aligned} \tag{32}$$

Equation (32) shows that for $\gamma_H \gg 1$ the subbarrier trajectory of the photoelectron is "pressed" to the electric field, contrary to the case of constant electric and magnetic fields, when for $\gamma_H \gg 1$ the subbarrier trajectory of the photoelectron is "pressed" to the magnetic field (see in Refs. [21,30]).

In the special case, when a right circularly polarized laser beam ($g = +1$) propagates parallel ($\theta = 0$) to the constant magnetic field $\boldsymbol{H}$, i.e., at $\mathcal{G}(g,\theta) = 2$, the emission angle of the photoelectron is

$$\varphi \to -\frac{\pi}{2} - \frac{\exp\left(\gamma_H^2/2\right)}{\gamma_H^2}\theta, \tag{33}$$

i.e., the photoelectron moves in the opposite direction to the electric field. In the case, when a left circularly polarized laser beam ($g = -1$) propagates parallel ($\theta = 0$) to the constant magnetic field $\boldsymbol{H}$, i.e., at $\mathcal{G}(g,\theta) = 0$, the emission angle of

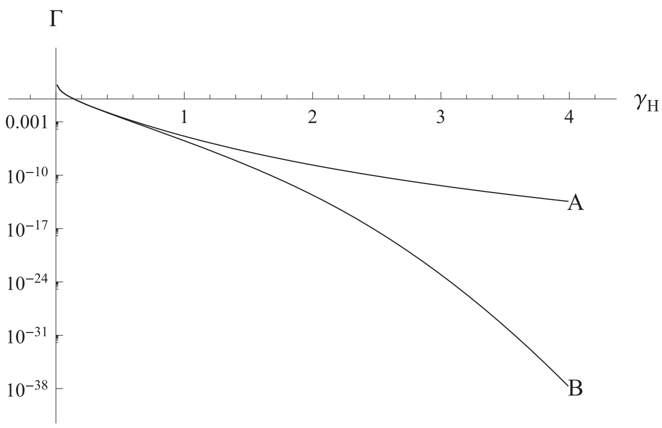

FIG. 1. Ionization rates Γ vs γ_H for the 1s state of the H atom ($\lambda_H \approx 8.77$) at $\theta = 0$, $g_A = -1$, and $g_B = +1$. Arbitrary units are used for Γ.

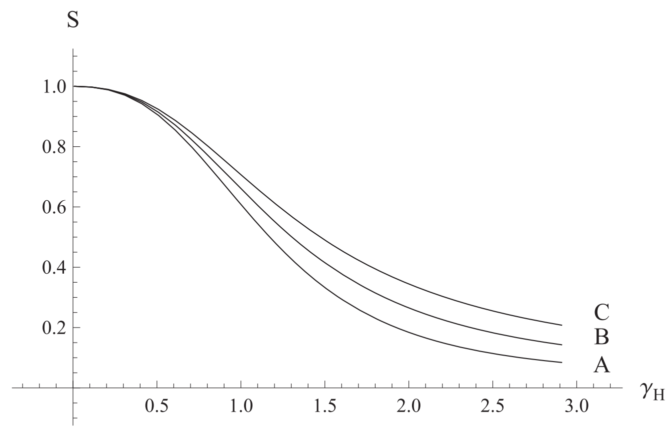

FIG. 2. Function S vs γ_H for the 1s state of the H atom ($\lambda_H \approx 8.77$) at $\theta = \pi/3$, $g_A = +1$, $g_B = +0.8$, and $g_C = +0.6$.

the photoelectron reads

$$\varphi \to \frac{\pi}{2} - \theta, \tag{34}$$

i.e., the photoelectron moves along the direction of the electric field.

IV. NUMERICAL CALCULATIONS

Figure 1 shows the ionization rates for the H atom in the field of a titanium-sapphire laser ($\omega = 1.55$ eV, $\lambda \approx 800$ nm) for intensity $J = 10^{13}$ W/cm^2, in the case when a left circularly polarized laser beam ($g_A = -1$) and a right circularly polarized laser beam ($g_B = +1$), with the frequencies $\omega = \omega_H$, propagate parallel ($\theta = 0$) to the constant magnetic field $\boldsymbol{H}$. Note that the cyclotron frequency $\omega_H = 1.55$ eV corresponds to the constant magnetic field $H \sim 134$ MG. As can be seen from Fig. 1 the ionization rate for a left polarized laser field is greater than for a right polarized laser field. The reason for this is that since a left circularly polarized laser pulse ($g = -1$) rotates the electron against the constant magnetic field, the subbarrier trajectory of the electron becomes shorter than in the case of a right circularly polarized laser field ($g = +1$). As a result the ionization rate for a left polarized field is greater than for a right polarized field.

Let us define the stabilization factor $S(\gamma_H, g, \theta)$: $S(\gamma_H, g, \theta) = \Gamma/\Gamma_0$, where Γ_0 is the ionization rate at $\boldsymbol{H} = \boldsymbol{0}$. In Refs. [21,30,40], it was shown that accounting for the constant magnetic field in the ionization process always leads to stabilization of a bound level. This is a fairly general statement well known in the literature for the atomic ionization. The stabilization effect can be explained by the distortion (elongation) of the subbarrier trajectory due to the screwlike electron motion in the magnetic field. Figures 2–6 show the results of numerical calculations in the field of a titanium-sapphire laser for the stabilization factor $S(\gamma_H, g, \theta)$, which determines the extent of the influence of the constant magnetic field on the ionization rate, in the case of neutral atoms of H and He. Note that numerical calculations (Figs. 1–6) were carried out in the framework of the zero-range potential model [see Eq. (5)], with binding energies corresponding to hydrogen and helium. Figure 2 shows that in the case of a right polarized laser field ($g > 0$) the stabilization factor decreases as the magnetic Keldysh parameter γ_H increases (as the magnetic field increases), i.e., the constant magnetic field stabilizes the bound level. This means that for a right polarized laser field, when the constant magnetic field and the electromagnetic wave rotate the electron in the same direction, the subbarrier trajectory of the electron elongates and the ionization probability, in the presence of the magnetic field, decreases as compared to the case when the magnetic field is absent. This stabilization effect increases with the ellipticity $g > 0$ and reaches a maximum for a right circularly polarized wave ($g = +1$).

Figures 3–6 show that in the case of a left polarized laser field ($g < 0$) the stabilization factor increases with the magnetic Keldysh parameter γ_H, i.e., with the magnetic field. This means that the ionization rate, in the presence of the magnetic field, is greater than when the magnetic field is absent. For a left polarized laser field, when the constant magnetic field and the electromagnetic wave, under the condition $\omega = \omega_H$, rotate the electron in the opposite directions, the subbarrier trajectory of the electron shortens as compared to the case when the magnetic field is absent. The consequence of this is

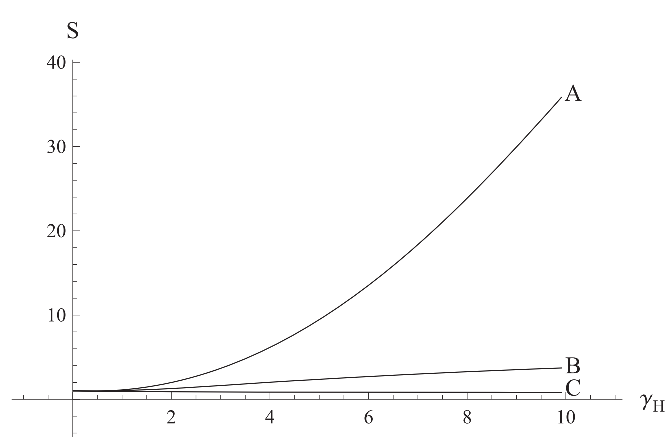

FIG. 3. Function S vs γ_H for the 1s state of the H atom ($\lambda_H \approx 8.77$) at $\theta = 0$, $g_A = -1$, $g_B = -0.8$, and $g_C = -0.6$.

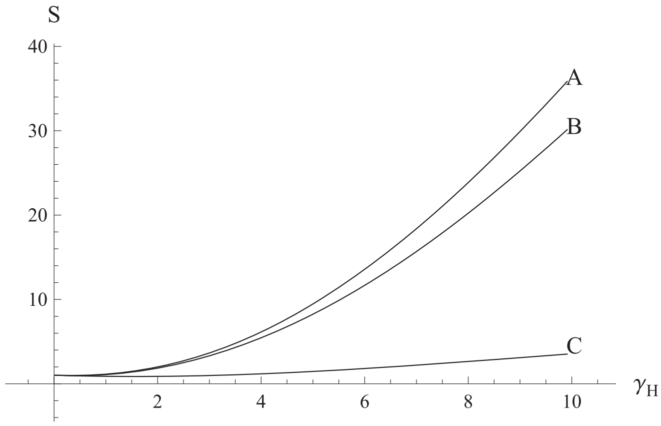

FIG. 4. Function S vs γ_H for the 1s state of the H atom ($\lambda_H \approx$ 8.77) at $g = -1$, $\theta_A = 0$, $\theta_B = \pi/4$, and $\theta_C = \pi/2$.

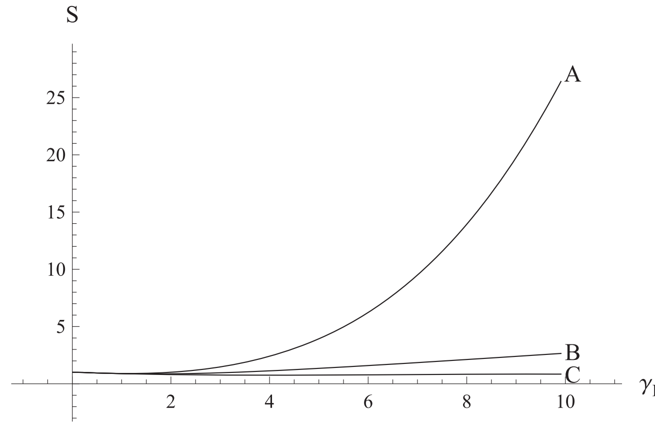

FIG. 6. Function S vs γ_H for the 1s state of the He atom ($\lambda_H \approx$ 15.8) at $\theta = \pi/2$, $g_A = \pm1$, $g_B = \pm0.8$, and $g_C = \pm0.6$.

that the constant magnetic field does not stabilize the bound level. It follows from Fig. 3 that the enhancement of the ionization rate in the constant magnetic field, when $\omega = \omega_H$, increases with the magnitude of the ellipticity $|g|$ and reaches a maximum in the case of a left circularly polarized laser pulse ($g = -1$). As can be seen from Figs. 4 and 5, the enhancement of the ionization rate increases as the angle between the magnetic field and the direction of a laser beam propagation approaches zero. This enhancement is maximal when a left circularly polarized laser beam propagates parallel ($\theta = 0$) to the magnetic field. In addition, these figures show that the enhancement of ionization rates for helium is greater than for hydrogen, because the magnetic multiquantum parameter λ_H for the He atom is greater than that for the H atom. Figure 6 shows that when a laser beam propagates perpendicularly ($\theta = \pi/2$) to the constant magnetic field, the enhancement of ionization rates does not depend on a sign of the laser field polarization and it is maximal for a circularly polarized laser pulse ($g = \pm1$).

V. CONCLUSIONS

We have considered the tunneling and multiphoton ionization of a weakly bound level in an intense monochromatic laser beam of an arbitrary polarization propagating at an arbitrary angle to a constant uniform magnetic field, under the condition when the frequency ω of a laser field coincides with the cyclotron frequency ω_H. Within the framework of the QQES formalism we have derived the equation for the complex quasienergy and expressions for ionization rates in the case of arbitrary magnitudes of the magnetic Keldysh parameter. Using the quasiclassical perturbation theory and the imaginary-time method we have also derived the extremal subbarrier trajectory of the electron. We analyzed in detail analytical expressions for ionization rates, the barrier width, and the emission angle of photoelectrons, in the tunneling and the multiphoton limits.

We have complemented our consideration by numerical calculations of ionization rates and stabilization factors for H and He atoms in the field of a titanium-sapphire laser. Our calculations showed the fundamental difference between the processes of the ionization in the fields of right and left polarized laser pulses, in the presence of the constant magnetic field, in the case when $\omega = \omega_H$. From our calculations, it follows that the ionization rate in the case of a left polarized laser field is greater than in the case of a right polarized laser field. The reason for this is the fact that since a right polarized electromagnetic wave and the constant magnetic field rotate the electron in the same direction, the subbarrier trajectory of the electron elongates. At the same time, a left polarized laser field rotates the electron against the constant magnetic field and the electron subbarrier trajectory becomes shorter. As a result a counterrotating electron has significantly better chances to penetrate the barrier than a corotating electron. The consequence of this is that for a right polarized electromagnetic wave the constant magnetic field always stabilizes the bound level. On the contrary, for a left polarized electromagnetic wave, under the condition $\omega = \omega_H$, the constant magnetic field does not stabilize the bound level, which leads to an enhancement of the ionization rate as compared to the case when the magnetic field is absent. Our calculations also showed that this enhancement of the ionization rate is maximal in the case of a left circularly polarized laser beam, propagating parallel to the magnetic field. The results obtained in this paper allow us to suggest using the constant magnetic field in a two-color scheme with

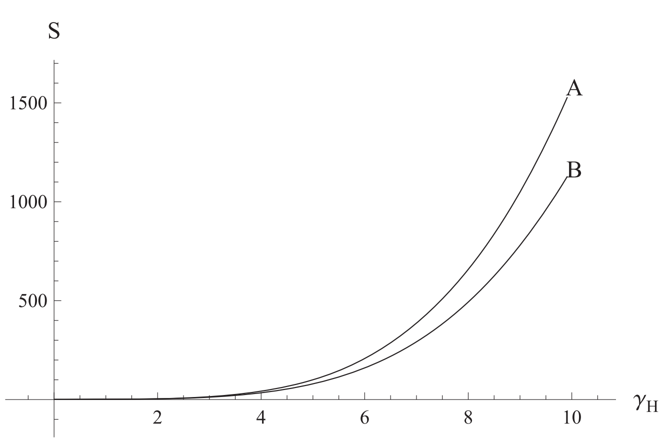

FIG. 5. Function S vs γ_H for the 1s state of the He atom ($\lambda_H \approx$ 15.8) at $g = -1$, $\theta_A = 0$, and $\theta_B = \pi/4$.

circular laser fields (see in Ref. [53]) when the frequency of one of the harmonics coincides with the cyclotron frequency, for an amplification of terahertz radiation.

ACKNOWLEDGMENT

I am deeply grateful to A. L. Mitler for performing numerical calculations.

[1] P. B. Corkum, N. H. Burnett, and F. Brunel, Phys. Rev. Lett. **62**, 1259 (1989).
[2] G. F. Gribakin and M. Yu. Kuchiev, Phys. Rev. A **55**, 3760 (1997).
[3] V. D. Mur, S. V. Popruzhenko, and V. S. Popov, Zh. Eksp. Teor. Fiz. **119**, 893 (2001) [JETP **92**, 777 (2001)].
[4] N. L. Manakov, M. V. Frolov, B. Borca, and A. F. Starace, J. Phys. B: At. Mol. Opt. Phys. **36**, R49 (2003).
[5] H. R. Reiss, Phys. Rev. Lett. **101**, 043002 (2008).
[6] H. R. Reiss, Phys. Rev. Lett. **102**, 143003 (2009).
[7] H. R. Reiss, Phys. Rev. A **82**, 023418 (2010).
[8] I. Barth and O. Smirnova, Phys. Rev. A **84**, 063415 (2011).
[9] I. Barth and O. Smirnova, Phys. Rev. A **87**, 013433 (2013).
[10] M. V. Frolov, D. V. Knyazeva, N. L. Manakov, J.-W. Geng, L.-Y. Peng, and A. F. Starace, Phys. Rev. A **89**, 063419 (2014).
[11] M. Klaiber, K. Z. Hatsagortsyan, and C. H. Keitel, Phys. Rev. Lett. **114**, 083001 (2015); **115**, 079904 (2015).
[12] M. Ohmi, O. I. Tolstikhin, and T. Morishita, Phys. Rev. A **92**, 043402 (2015).
[13] J. M. Ngoko Djiokap, A. V. Meremianin, N. L. Manakov, S. X. Hu, L. B. Madsen, and A. F. Starace, Phys. Rev. A **94**, 013408 (2016).
[14] M. V. Frolov, N. L. Manakov, A. A. Minina, S. V. Popruzhenko, and A. F. Starace, Phys. Rev. A **96**, 023406 (2017).
[15] D. B. Milošević, Phys. Rev. A **98**, 033405 (2018).
[16] S. Luo, M. Li, W. Xie, K. Liu, Y Feng, B Du, Y. Zhou, and P. Lu, Phys. Rev. A **99**, 053422 (2019).
[17] O. I. Tolstikhin and T. Morishita, Phys. Rev. A **99**, 063415 (2019).
[18] L. V. Keldysh, Zh. Eksp. Teor. Fiz. **47**, 1945 (1964) [Sov. Phys. JETP **20**, 1307 (1965)].
[19] L. I. Kotova, A. M. Perelomov, and V. S. Popov, Zh. Eksp. Teor. Fiz. **54**, 1151 (1968) [Sov. Phys. JETP **27**, 616 (1968)].
[20] V. S. Popov and A. V. Sergeev, Pis'ma Zh. Eksp. Teor. Fiz. **63**, 398 (1996) [JETP Lett. **63**, 417 (1996)].
[21] V. S. Popov, B. M. Karnakov, and V. D. Mur, Zh. Eksp. Teor. Fiz. **113**, 1579 (1998) [JETP **86**, 860 (1998)].
[22] N. L. Manakov and A. G. Fainshtein, Dokl. Akad. Nauk SSSR **244**, 567 (1979) [Sov. Phys. Doklady **24**, 41 (1979)].
[23] N. L. Manakov and A. G. Fainshtein, Zh. Eksp. Teor. Fiz. **79**, 751 (1980) [Sov. Phys. JETP **52**, 382 (1980)].
[24] Y. B. Zel'dovich, Usp. Fiz. Nauk **110**, 139 (1973) Ya. B. Zel'dovich, [Sov. Phys. Usp. **16**, 427 (1973)].
[25] Y. B. Zel'dovich, N. L. Manakov, and L. P. Rapoport, Usp. Fiz. Nauk **117**, 569 (1975) [Sov. Phys. Usp. **18**, 920 (1975)].
[26] N. L. Manakov, M. A. Preobrazhenskii, L. P. Rapoport, and A. F. Fainshtein, Zh. Eksp. Teor. Fiz. **75**, 1243 (1978) [Sov. Phys. JETP **48**, 626 (1978)].
[27] M. V. Frolov, A. V. Flegel, N. L. Manakov, and A. F. Starace, Phys. Rev. A **75**, 063407 (2007).
[28] M. V. Frolov, A. V. Flegel, N. L. Manakov, and A. F. Starace, Phys. Rev. A **75**, 063408 (2007).
[29] M. V. Frolov, N. L. Manakov, and A. F. Starace, Phys. Rev. A **78**, 063418 (2008).
[30] V. M. Rylyuk, Phys. Rev. A **93**, 053404 (2016).
[31] V. M. Rylyuk and J. Ortner, Phys. Rev. A **67**, 013414 (2003).
[32] V. M. Rylyuk, Phys. Rev. A **86**, 013402 (2012).
[33] N. B. Delone and V. P. Krainov, Usp. Fiz. Nauk **168**, 531 (1998) [Sov. Phys. Usp. **41**, 469 (1998)].
[34] V. S. Popov, Usp. Fiz. Nauk **174**, 921 (2004) [Sov. Phys. Usp. **47**, 855 (2004)].
[35] W. Becker, X. J. Liu, P. J. Ho, and J. H. Eberly, Rev. Mod. Phys. **84**, 1011 (2012).
[36] S. V. Popruzhenko, J. Phys. B: At. Mol. Opt. Phys. **47**, 204001 (2014).
[37] B. M. Karnakov, V. D. Mur, S. V. Popruzhenko, and V. S. Popov, Usp. Fiz. Nauk **185**, 3 (2015) [Sov. Phys. Usp. **58**, 3 (2015)].
[38] V. S. Popov, V. S. Kuznetsov, and A. M. Perelomov, Zh. Eksp. Teor. Fiz. **53**, 331 (1967) [Sov. Phys. JETP **26**, 240 (1968)].
[39] V. S. Popov, Yad. Fiz. **68**, 717 (2005) [Phys. At. Nucl. **68**, 686 (2005)].
[40] V. M. Rylyuk, Eur. Phys. J. D **72**, 218 (2018).
[41] A. D. Sakharov *et al.*, Dokl. Akad. Nauk SSSR **165**, 65 (1965).
[42] A. D. Sakharov, Usp. Fiz. Nauk **88**, 725 (1966) [Sov. Phys. Usp. **9**, 294 (1966)].
[43] G. Sarri, A. Macchi, C. A. Cecchetti, S. Kar, T. V. Liseykina, X. H. Yang, M. E. Dieckmann, J. Fuchs, M. Galimberti, L. A. Gizzi *et al.*, Phys. Rev. Lett. **109**, 205002 (2012).
[44] M. Tatarakis, I. Watts, F. Beg *et al.*, Nature **415**, 280 (2002).
[45] M. Tatarakis *et al.*, Phys. Plasmas **9**, 3642 (2002).
[46] U. Wagner *et al.*, Phys. Rev. E **70**, 026401 (2004).
[47] I. Seipp and W. Schweizer, Astron. Astrophys. **318**, 990 (1997).
[48] I. Seipp, K. T. Taylor, and W. Schweizer, J. Phys. B **29**, 1 (1996).
[49] Y. N. Demkov and G. F. Drukaryev, Zh. Eksp. Teor. Fiz. **47**, 918 (1964) [Sov. Phys. JETP **20**, 614 (1965)].
[50] Y. N. Demkov and V. N. Ostrovsky, *Zero–Range Potentials and Their Application in Atomic Physics* (Plenum Press, NY, 1988).
[51] L. D. Landau and E. M. Lifshitz, *Quantum Mechanics*, 4th ed. (Pergamon, Oxford, 1992).
[52] L. D. Landau, Phys. Z. Sowjetunion **1**, 88 (1932); **2**, 46 (1932); *Collected Works* (Nauka, Moscow, 1969), Vol.1.
[53] C. Meng, W. Chen, X. Wang, Z. Lü, Y. Huang, J. Liu, D. Zhang, Z. Zhao, and J. Yuan, Appl. Phys. Lett. **109**, 131105 (2016).